

Purely stochastic binary decisions in cell signaling models without underlying deterministic bistabilities

Maxim N. Artyomov*, Jayajit Das†, Mehran Kardar‡, and Arup K. Chakraborty*†§¶

Departments of †Chemical Engineering, *Chemistry, ‡Biological Engineering, and †Physics, Massachusetts Institute of Technology, Cambridge, MA 02139

Edited by Mark A. Ratner, Northwestern University, Evanston, IL, and approved September 27, 2007 (received for review June 28, 2007)

Detection of different extracellular stimuli leading to functionally distinct outcomes is ubiquitous in cell biology, and is often mediated by differential regulation of positive and negative feedback loops that are a part of the signaling network. In some instances, these cellular responses are stimulated by small numbers of molecules, and so stochastic effects could be important. Therefore, we studied the influence of stochastic fluctuations on a simple signaling model with dueling positive and negative feedback loops. The class of models we have studied is characterized by single deterministic steady states for all parameter values, but the stochastic response is bimodal; a behavior that is distinctly different from models studied in the context of gene regulation. For example, when positive and negative regulation is roughly balanced, a unique deterministic steady state with an intermediate value for the amount of a downstream signaling product is found. However, for small numbers of signaling molecules, stochastic effects result in a bimodal distribution for this quantity, with neither mode corresponding to the deterministic solution; i.e., cells are in “on” or “off” states, not in some intermediate state. For a large number of molecules, the stochastic solution converges to the mean-field result. When fluctuations are important, we find that signal output scales with control parameters “anomalously” compared with mean-field predictions. The necessary and sufficient conditions for the phenomenon we report are quite common. So, our findings are expected to be of broad relevance, and suggest that stochastic effects can enable binary cellular decisions.

bimodality | fluctuations

The detection of external stimuli by receptors on a cell membrane followed by intracellular signaling, gene transcription, and effector functions is ubiquitous, and necessary for life. The regulatory processes involved in gene transcription are often mediated by small numbers of molecules. This makes stochastic effects important and, in recent years, many interesting consequences of such fluctuations have been elucidated theoretically and observed in experiments (e.g., refs. 1–4). The importance of stochastic effects on enzymatic reactions in the zero order ultrasensitivity regime has also been described (5, 6). Less attention has been devoted to the effects of stochastic fluctuations on cell signaling dynamics. However, many such processes involve small numbers of molecules. One important example is provided by T lymphocytes (T cells), the orchestrators of the adaptive immune response. T cell signaling and activation can be stimulated by as few as three molecules that represent signatures of pathogens (called agonists) (7–12). The small numbers of molecules involved can make stochastic effects important for membrane-proximal signaling in T cells. Here, we study simple and general models inspired by recent descriptions of membrane-proximal signaling in T cells, and find an interesting consequence of stochastic fluctuations. An essential feature of the model, dueling positive and negative feedback loops, is ubiquitous, and so our findings may be of broad relevance in cell biology.

Many examples (particularly models of gene regulation) have been studied wherein a deterministic treatment of the kinetic scheme describing the relevant processes has two stable steady

states in a certain parameter regime (1–3, 13, 14). In such systems, stochastic effects can lead to bimodality (e.g., populated “on” and “off” states) in the parameter range where bistability is predicted by the deterministic equations as well as outside this range where there is a single stable steady state (1–3, 13, 14). The latter phenomenon is a consequence of stochastic fluctuations enabling the system to sample parameters (e.g., rate constants) that effectively fall within the range where two deterministically stable fixed points are present. In these examples, the existence of bistability in the deterministic analysis in some parameter range underlies the observation of bimodal behavior in the stochastic treatment.

The model we study exhibits a different feature. The deterministic dynamical equations yield a single steady state in all parameter ranges; i.e., there is no bistability. Yet, stochastic fluctuations result in a bimodal long-time response with neither mode corresponding to the steady state obtained deterministically. Upon increasing the copy numbers of molecules, the stochastic description ultimately converges to the deterministic behavior. Thus, we find a purely stochastically driven instability when none exists in the deterministic treatment in any parameter range. When fluctuations are important, we find that average quantities scale with parameters “anomalously” compared with the corresponding mean-field behavior. Our analyses suggest that the necessary and sufficient conditions for this phenomenon to occur are quite common.

Signaling Model

Our simple (“toy”) model is inspired by ideas proposed recently to describe T cell responses to diverse stimuli (7–9, 15–17). T cell receptor (TCR) molecules expressed on the surface of T cells can bind complexes of peptides (p) bound to MHC proteins on the surface of antigen-presenting cells (APCs). TCR can potentially bind strongly to pMHC molecules where the peptide is derived from a pathogen’s proteins (agonists). In contrast, thymic selection ensures that TCR bind weakly to “self” or endogenous pMHC molecules that are also expressed on APCs (18). The binding of TCRs to pMHC molecules can initiate signaling cascades that result in T cell activation and an immune response. T cells are as good a sensory apparatus as any in biology, and can detect as few as three agonists in a sea of tens of thousands of endogenous pMHC molecules, and it has been suggested that this extraordinary sensitivity is mediated by cooperative interactions between self pMHC and agonists (7–10, 19).

Another interesting response of T cells to pMHC molecules is called antagonism (15, 20). Antagonists are pMHC molecules obtained by mutating agonist peptide residues. When present on

Author contributions: M.N.A., J.D., and A.K.C. designed research; M.N.A. and J.D. performed research; M.N.A., J.D., M.K., and A.K.C. analyzed data; and M.N.A., J.D., M.K., and A.K.C. wrote the paper.

The authors declare no conflict of interest.

Abbreviation: TCR, T cell receptor.

¶To whom correspondence should be addressed. E-mail: arupc@mit.edu.

This article contains supporting information online at www.pnas.org/cgi/content/full/0706110104/DC1.

© 2007 by The National Academy of Sciences of the USA

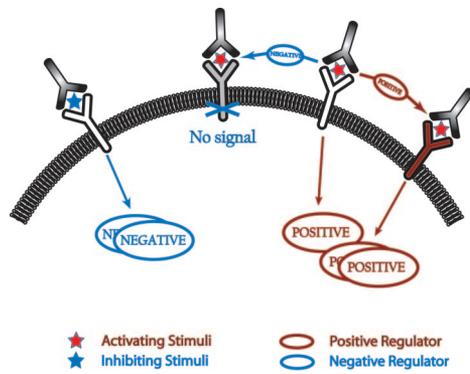
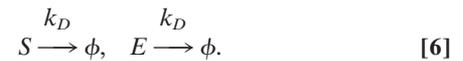
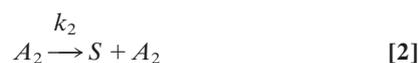


Fig. 1. A schematic representation of dueling positive and negative feedback loops stimulated upon receptor binding to stimulatory or inhibitory ligands. The negative regulator can shut off signaling by inactivating the receptor-associated signaling complex (negative feedback), whereas the positive regulator could prevent this inhibitory interaction and increase or continue production of downstream signaling products (positive feedback).

APC surfaces in sufficient numbers, they can shut down intracellular signaling stimulated in response to agonists. Recent experimental results (15) have suggested that this phenomenon may be mediated by dueling positive and negative feedback loops (Fig. 1). One of the earliest steps in downstream signaling initiated by the binding of the TCR to pMHC molecules is the phosphorylation of cytoplasmic domains of the TCR complex by a kinase called Lck. It has been proposed that Lck also activates its own inhibitor, a phosphatase called Shp (negative feedback). This inhibitory interaction is prevented by a product (ERK) of signaling downstream of phosphorylation of the TCR complex that protects Lck by phosphorylating one of its sites (positive feedback). It has been proposed, and supported by detailed calculations (16, 17), that the positive feedback is dominant when T cells are stimulated by agonists (and synergistic endogenous ligands), and negative feedback shuts down signaling when sufficient numbers of antagonists are present.

Although the specific molecular identity of positive and negative regulators involved in T cell signaling is still debated (21), the idea that dueling positive and negative feedback loops play a role in determining whether signaling is shut off (antagonism) or sustained/amplified (agonism) is of general significance to cellular decisions that lead to distinct outcomes. Furthermore, such processes are often mediated by small numbers of molecules. Therefore, we set out to study the effects of stochastic fluctuations on the following simple and general model with dueling positive and negative feedback regulation



Although this model is general, seeing how it relates to T cell signaling makes clear that it is relevant to situations where cells make distinct decisions (e.g., agonism and antagonism in Fig. 1). Reaction 1 mimics the production of the positive regulator ERK (E) upon agonist (A_1) binding to TCR. Thus, it subsumes a large number of steps in the actual signaling cascade into one. Of course, agonists also lead to production of the negative regulator Shp (S), but this is ignored in this general model. Similarly, some production of E by antagonist (A_2) binding to the receptor is ignored, and reaction 2 mimics the production of the negative regulator. Reaction 3 represents positive feedback and mimics protection of Lck from the action of Shp, in that the interaction of E with A_1 protects it (by forming A_1^{PROT}) from the inhibitory action of S (reaction 5). Protected A_1 species can generate positive regulators E (reaction 4), and both positive and negative regulators can be inactivated (reaction 6).

Results

The mean-field deterministic equations corresponding to the model described by Eqs. 1–6 can be written down following mass action kinetics [supporting information (SI) Text, SI Table 1, and SI Figs. 6–9], and yield the following solution for the steady state:

$$A_1^{(\text{SS})} = 0, \quad A_1^{\text{PROT}(\text{SS})} + A_1^{\text{INACTIV}(\text{SS})} = A_{1,\text{initial}},$$

$$E^{(\text{SS})} = \frac{k_4}{k_D} A_1^{\text{PROT}(\text{SS})}, \quad S^{(\text{SS})} = \frac{k_2}{k_D} A_2. \quad [7]$$

At steady state, the number of A_1 molecules equals zero, the number of S molecules is a function of the number of A_2 molecules, the number of E molecules depends on the number of protected A_1 molecules, and all solutions that satisfy the constraint that the sum of the number of A_1^{PROT} species and A_1^{INACTIV} species sum to the initial number of A_1 are allowed. Thus, unique steady states cannot be obtained from Eqs. 7 without knowledge of the initial conditions. Rather, there is a line of possible steady states. Stability analysis shows that all, but one, eigenvalues of the Jacobian matrix are negative. The only nonnegative eigenvalue is zero, and corresponds to sliding along the line of possible steady states, $A_1^{\text{PROT}(\text{SS})} + A_1^{\text{INACTIV}(\text{SS})} = A_{1,\text{initial}}$, with corresponding change in the steady-state value of E . Solving the dynamical equations with specific initial conditions and taking the long-time limit obtains a unique point on this fixed line. Thus, the deterministic solutions of the model are a set of unique steady-states for all parameter values.

Although we have studied different parameter ranges for a stochastic description of this model (SI Text), let us first consider situations that are inspired by T cell signaling. Reactions 1, 2, and 4 represent multistep processes (22). Reactions 3 and 5, the dueling feedback loops, are thought to represent one-step phosphorylation or deactivation steps (15). So, we study situations where k_3 and k_5 are much larger than k_1 , k_2 , and k_4 ; i.e., both positive and negative feedback loops are strong. Recent studies (9, 17) with detailed models of membrane-proximal signaling in T cells suggests that k_4 could be larger than k_1 , but we have taken them to be equal ($k_4 > k_1$ is considered in the SI Text). Changing the relative values of k_1 and k_2 would simply modify the specific value of the ratio of initial numbers of A_1 and A_2 molecules that would result in a transition from “agonism” to “antagonism.”

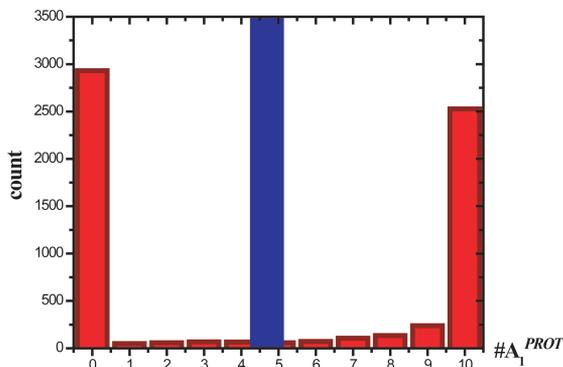


Fig. 2. Bimodal stochastic solutions distinct from the unique deterministic solution. Histogram showing the bimodal distribution of the protected agonists at steady state (red) for a situation when there are 10 agonist (A_1) and 10 antagonists (A_2). The corresponding single steady state solution of the deterministic ODEs (blue) is also shown. The other parameter values are: $k_1 = 1$, $k_2 = 1$, $k_3 = 100$, $k_4 = 1$, $k_5 = 100$, $k_D = 1$ (all s^{-1}), and statistics were collected over 5,000 trajectories obtained by using the Gillespie algorithm. The result is robust to variations in the parameter values as long as there is strong feedback.

Fig. 2 shows results of spatially homogeneous stochastic simulations with discrete number of molecules [using the Gillespie algorithm (23)] of the model represented by Eqs. 1–6. When there are only a few molecules of A_1 and A_2 , essentially all of the stochastic trajectories commit to one of two final states: all of the A_1 molecules are converted to the protected species, A_1^{PROT} , or are annihilated and signaling stops. This bimodality is in striking contrast to the mean-field solution that does not exhibit bistability for any parameter values. The qualitative phenomenon of finding a bimodal stochastic solution when the deterministic solution is unique for all parameter values is preserved as long as the positive and negative feedback loops are sufficiently strong (SI Text).

The mechanism underlying this result is as follows. The species A_1 is converted to either A_1^{PROT} or A_1^{INACT} . The effective rates of production of these species can be obtained from the deterministic equations. Both rates equal zero initially and at long times, and exhibit a maximum (SI Fig. 9). The initial rise and amplitudes of the maxima depend on the values of the initial number of A_1 and A_2 molecules, and are very different if one of these quantities is much larger than the other. In these circumstances, either agonism or antagonism dominates in the deterministic and stochastic solutions. The more interesting cases are ones where the generation of positive and negative regulations is roughly balanced (Fig. 2) because it could result in a transition from agonism to antagonism. Now, the rates at short times and amplitudes of the maxima for the production of A_1^{PROT} and

A_1^{INACT} are comparable in the mean-field sense, and the deterministic equations yield a single steady state solution with an intermediate value of A_1^{PROT} . However, stochastically, one of two reactions 1 and 2 occurs first. There is a stochastic delay, τ , before the other reaction occurs, and for this duration, the reaction propensities are effectively as in cases where $A_1 \gg A_2$, or vice versa. For small numbers of A_1 and A_2 molecules, τ can be long. If τ is longer than the intrinsic time scale associated with the feedback reaction corresponding to the reaction that occurred first (e.g., reaction 3 if 1 occurred first), then the small number of A_1 molecules will all be converted to either A_1^{PROT} or be annihilated, depending upon whether reaction 1 or 2 occurred first. So, the stochastic trajectories partition into two classes (those that end with all A_1 molecules annihilated or protected), and the stochastic solution is bimodal.

The time delay (τ) becomes smaller as the number of molecules of A_1 and A_2 increases. This observations suggests that, for a sufficiently large number of particles, it will not be longer than the intrinsic time scale associated with the feedback loops and the stochastic solution will not be bimodal. Rather, it will be distributed around the mean-field solution. Fig. 3 shows results of simulations that demonstrate this unequivocally. Thus, for the same parameter values, as the number of molecules decreases past a threshold, the stochastic solution exhibits an instability from one solution to bimodality. This transition from unimodal to bimodal solutions is driven by stochastic effects, and occurs in the absence of any underlying deterministic bistability.

The qualitative differences between the stochastic and deterministic descriptions due to the dominance of fluctuation effects suggests that the manner in which the response scales with different control parameters may be different. For example, we expect the steady state amount of A_1^{PROT} to scale with $k_1 A_1 / k_2 A_2$ for the stochastic simulations. This is because the probability of conversion to A_1^{PROT} is essentially equal to the probability that reaction 1 occurs first, which is given by $k_1 A_1 / (k_1 A_1 + k_2 A_2)$. Conversely, probability of annihilating all A_1 molecules is equal to $k_2 A_2 / (k_1 A_1 + k_2 A_2)$ (equal to probability that reaction 2 occurs first). Both expressions depend only on the combination $k_1 A_1 / k_2 A_2$. This implies, for example, that the amount of A_1^{PROT} scales linearly with k_1 (a measure of how effective the agonist is in stimulating signaling). The deterministic solution, on the other hand, is not expected to obey this linear scaling. Indeed, numerical solutions support these expectations (SI Fig. 8).

The complexity of the model described by Eqs. 1–6, however, makes it difficult to explore these differences in scaling behavior precisely. The complexity also prevents us from analyzing the necessary and sufficient conditions for purely stochastic instabilities (results in Figs. 2 and 3) in cell signaling dynamics. Therefore, we formulated a simpler model that enabled exploration of these issues.

This minimal model, which can be solved exactly, includes the following features: irreversibility, branching, and feedback. The

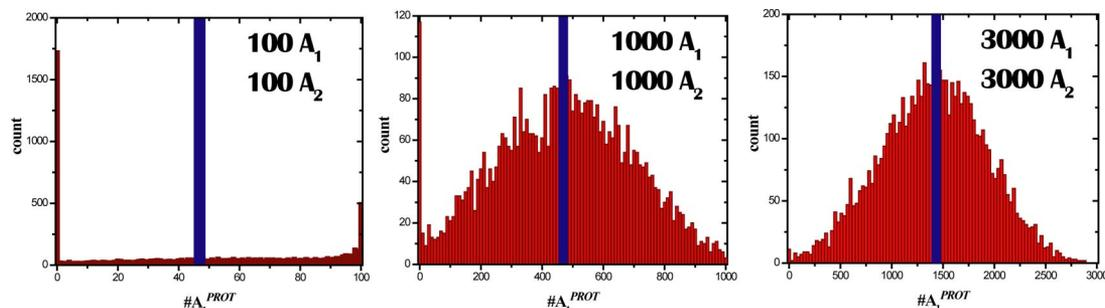
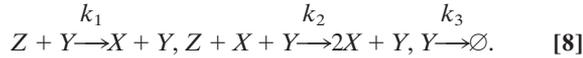


Fig. 3. A purely stochastically driven transition. Histograms showing the distribution of the protected agonists at steady state (red) and corresponding steady state solution of deterministic ODEs (blue) for different amounts of agonist and antagonist. All other parameters are identical to that in Fig. 2.

model is described in terms of the three coupled reactions shown below:



The deterministic equations corresponding to these reactions can be written down (SI Text) following the mass action kinetics. Let us denote the numbers of x , y , and z species at time t by $N_x(t)$, $N_y(t)$, and $N_z(t)$, respectively. At $t = 0$, only Z and Y species are present; i.e., $N_x(0) = 0$, $N_y(0) = N$, and $N_z(0) = M$. As for the more complex model, the steady state values of the numbers of each species cannot be determined by setting the right sides of the above rate equations to zero; i.e., only a line of possible steady states can be obtained. Linear stability analysis of the steady state solutions shows that there is a neutral mode (with an eigenvalue 0) corresponding to sliding along the line of possible steady states, and stable modes along the directions $\delta N_x + (k_2 N_x^s + k_1)(M - N_x^s)/k_3 \delta N_y$ and δN_y , respectively, which span the plane of the steady states. It is easy to solve the time dependent equations and take the $t \rightarrow \infty$ limit to obtain the unique steady-state solution for given initial conditions. The time-dependent solution to the deterministic equations describing system (8) is:

$$N_x(t) = \frac{k_1 M(F(t) - 1)}{Mk_2 + k_1 F(t)}, \quad N_y(t) = N e^{-k_3 t}, \quad N_z(t) = M - N_x(t), \quad [9]$$

where $F(t) = \exp[(Mk_2 + k_1)N(1 - e^{-k_3 t})/k_3]$. At long times ($t \gg k_3^{-1}$), the steady state particle numbers are

$$N_x(t \rightarrow \infty) = N_x^s = \frac{k_1 M(\exp[N(Mk_2 + k_1)/k_3] - 1)}{Mk_2 + k_1 \exp[N(Mk_2 + k_1)/k_3]} \quad [10]$$

$$N_y(t \rightarrow \infty) = N_y^s = 0, \quad N_z(t \rightarrow \infty) = N_z^s = M - N_x(t \rightarrow \infty). \quad [11]$$

Given initial conditions, these equations determine a unique steady state, a behavior identical to that exhibited by the model described by Eqs. 1–6. Unlike the more complex model, the deterministic scaling behavior can be determined, and is given by $N_x^s(k_1, k_2, k_3, N, M) = Mf(Mk_2 k_1^{-1}, Nk_1 k_3^{-1})$.

The following Master Equation describes the stochastic time evolution of the reactions shown in (8)

$$\frac{\partial P(n_x, n_y, n_z, t)}{\partial t} = [k_2(n_x - 1)n_y(n_z + 1) + k_1 n_y(n_z + 1)] P(n_x - 1, n_y, n_z + 1, t) + k_3(n_y + 1)P(n_x, n_y + 1, n_z, t) - (k_2 n_x n_y n_z + k_1 n_y n_z + k_3 n_y)P(n_x, n_y, n_z, t). \quad [12]$$

$P(n_x, n_y, n_z, t)$ denotes the probability of having n_x , n_y , and n_z particles at time t . The probability distribution at $t = 0$ is given by $P(n_x, n_y, n_z, t = 0) = \delta_{n_x,0} \delta_{n_y,N} \delta_{n_z,M}$. Note that, at steady state (or in the limit, $t \rightarrow \infty$), there will be no y species present, and therefore, $P(n_x, n_y, n_z, t \rightarrow \infty) = \phi(n_x, n_z) \delta_{n_y,0}$. However, any form of $\phi(n_x, n_z)$ will make the right hand side of Eq. 12 vanish. Therefore, as for the deterministic equations, irreversibility makes it necessary to solve the time-dependent Master equation for a particular initial condition to obtain the steady-state solution.

Using the method of generating functions (24), Eq. 12 can be solved exactly (SI Text) to obtain:

$$P(n_x, n_y, n_z, t) = \delta_{n_x+n_z, M} \sum_{r=n_z}^M \lambda_r p_{nr} {}^N C_{n_y} \left[\frac{k_3}{A_r + k_3} (1 - \exp(-(A_r + k_3)t)) \right]^{N-n_y} \exp(-n_y(A_r + k_3)t), \quad [13]$$

where $A_r = r((M - r)k_2 + k_1)$ and $p_{nr} = {}^r C_{n_z} (-1)^{n_z} \Gamma(M + k_1/k_2 + 1 - r) \Gamma(M + k_1/k_2 - n_z) / \Gamma(M + k_1/k_2 + 1 - n_z - r) \Gamma(M + k_1/k_2)$. $\{\lambda_r\}$ are determined from the equations

$$\sum_{r=n}^M \lambda_r p_{nr} = 0 \quad \text{for } n < M \\ = 1 \quad \text{for } n = M. \quad [14]$$

At long times ($t \rightarrow \infty$), the above probability distribution takes the form,

$$P(n_x, n_y, n_z, t \rightarrow \infty) = \delta_{n_x+n_z, M} \delta_{n_y, 0} \sum_{r=n_z}^M \lambda_r p_{nr} \left[\frac{k_3}{(r(M - r)k_2 + rk_1) + k_3} \right]^N. \quad [15]$$

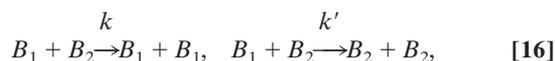
Note that this solution to the Master equation indicates the appearance of a spectrum of time scales (indexed by r and n_y), which is presumably related to stochastic delays.

Eq. 15 results in a steady state probability distribution that is bimodal for small numbers of molecules (SI Fig. 11a) when the deterministic solution does not exhibit bistability in any parameter range. In the more complex model that we studied (Eqs. 1–6), mean-field behavior was obtained as the numbers of A_1 and A_2 molecules increased past a threshold value even though their relative numbers were kept constant. The corresponding limit for the minimal model is $k_3 \rightarrow \infty$, $N \rightarrow \infty$, with the ratio N/k_3 (or the dimensionless, Nk_1/k_3) remaining constant. This is because a large value of N corresponds to a large amount of the source of a positive regulator (A_1 in Eqs. 1–6) and a large value of k_3 corresponds to greater annihilation or a big source (A_2 in Eqs. 1–6) of negative regulation. SI Fig. 11b shows that, like the more complex model, there is a purely stochastic transition as the stochastic solution is unimodal and distributed around the deterministic solution above a threshold value of N and k_3 . So, these results establish that the sufficient conditions for the phenomena we report are: irreversibility, branching, and feedback loops. But, are these also necessary conditions?

The possibility of two different outcomes is obviously necessary, and branching is ubiquitous in cell signaling processes that lead to functional decisions. We have also found that removing irreversibility abolishes the phenomenon (data not shown). Ultimately, all reactions are, in principle, reversible. However, in the time scales of interest to signal propagation in cells, many steps are effectively irreversible.

Feedback regulation is also necessary as the bimodal stochastic solution does not exist if k_2 in the minimal model tends to zero (SI Fig. 15). Insight into the kind of feedback regulation that is necessary can be obtained by contrasting our studies of dueling feedback loops in cell signaling to a model for binary drift in population genetics (25, 26). Consider a population of heterozygote individuals with two forms, B_1 and B_2 , for a particular allele. In the absence of mutations, the number of each type of allele can change from generation to generation, even in a population of fixed size, due to mating. The effects of binary

selection on the numbers of B_1 and B_2 forms can be roughly represented as follows (25, 26):



with k and k' related to the relative fitness of each phenotype.

The model described by Eq. 16 also contains branching and irreversibility. There is also an effective feedback, but unlike Eqs. 1–6 or 8, there is no separate intrinsic time scale associated with the feedback loops. A special case of this model (with no selection), $k = k'$, shares some features with the systems we are considering. The deterministic changes in this limit are trivially zero, and any initial condition (along the fixed line of $B_1 + B_2 =$ population size) remains fixed. These deterministic steady states are unique, but the stochastic solutions yield a bimodal distribution. This is because the stochastic trajectories are divided into two classes: ones that terminate when the number of B_1 particles vanishes and those that terminate when the number of B_2 reaches zero.

There is an important difference, however, between the model for binary drift with $k = k'$ and the class of cell signaling models we have been considering. The stochastic solution of the model represented by Eq. 16 does not converge to the deterministic solution when the number of particles becomes large. The stochastic solution at $t \rightarrow \infty$ is always bimodal. The stochastic trajectories cease to evolve when either B_1 or B_2 become zero because only then is the effective rate of conversion between these species equal to zero. The deterministic rates of formation of B_1 and B_2 equal the same constant for all times. Increasing the numbers of molecules does not eliminate this difference between the deterministic and stochastic cases. As the number of particles increases, the stochastically determined time (τ') required for B_1 or B_2 to equal zero increases, but ultimately it always happens. There is no separate intrinsic time scale that can compete with increasing values of τ' as the number of particles increases and prevent this from happening (i.e., a bimodal solution). Recall that, for the signaling models that we focused on, the relative values of the stochastic delay, τ , and the separate time scale associated with feedback loops determined the stochastically driven transition when the number of molecules was lowered (Fig. 3 and SI Fig. 11b). The absence of such an interplay prevents a purely stochastic instability in the binary drift model as the number of particles decreases. Correspondingly, if the rate coefficients in the model represented by Eq. 16 were time dependent with an intrinsic time scale, the phenomenon of a purely stochastic instability would be recovered.

The analyses presented above suggest that the necessary and sufficient conditions for a purely stochastic bimodality in the absence of any deterministic bistabilities are: (i) irreversibility, (ii) branching, and (iii) feedback regulation with an associated distinct and fast time scale.

The analytical solution for the probability distribution (Eq. 15) obtained for the minimal model of cell signaling that satisfies these conditions enables us to calculate average properties, such as the average number of molecules of the product, $\langle x \rangle$. This allows us to examine whether $\langle x \rangle$ scales with parameter values in the same way as N_x determined from the mean-field equations (see above). The average value, $\langle x \rangle$, is

$$\langle x \rangle = \sum_{n=0}^M \sum_{r=n}^M \lambda_r p_{nr} (M-n) \left(\frac{k_3}{r(M-r)k_2 + k_1 + k_3} \right)^N. \quad [17]$$

So, in general, there is no simple scaling law, such as N_x scaling with Nk_1/k_3 , as in the deterministic limit. Does this “anomalous” scaling, originating from the importance of stochastic fluctua-

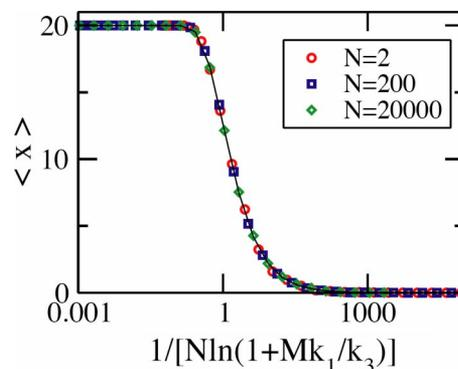


Fig. 4. Results from the minimal model. Non-mean-field scaling in the limit of large positive feedback ($k_2 \rightarrow \infty$): The average values of X species, $\langle x \rangle$, at steady state obtained from Gillespie simulations scale with $(1/\log(1 + Mk_1/k_3))$ instead of the mean field scaling variable Nk_1/k_3 . The values of the parameter k_2 is 100 s^{-1} (i.e., a large value). $k_1 = 0.0012 \text{ s}^{-1}$ and $M = 20$ are held fixed as k_3 and N are varied. The solid line is a plot of the scaling function shown in Eq. 19.

tions, revert to mean-field scaling behavior in the limit corresponding to a large numbers of particles?

To answer this question, as shown above, we need to consider the value of $\langle x \rangle$ in the limit of large values of N , M , and k_3 . Consider first the limit of large values of N and k_3 for a fixed value of Nk_1/k_3 . Simple algebra yields the value of $\langle x \rangle$ in this limit to be

$$\begin{aligned} \lim_{\substack{N \rightarrow \infty \\ k_3 \rightarrow \infty \\ k_3/N \text{ fixed}}} \langle x \rangle &= \sum_{n=0}^M \sum_{r=n}^M \lambda_r p_{nr} (M-n) \exp(-r((M-r)k_2/k_1 + 1)Nk_1/k_3). \end{aligned} \quad [18]$$

So, the deterministic scaling with Nk_1/k_3 (Eq. 10) is recovered in the appropriate limit. Similarly, mean-field scaling is recovered in the limit of large values of N and M (SI Text).

The general solution (Eq. 18) for $\langle x \rangle$ does not allow us to explicate the non-mean-field scaling when fluctuations are important. This can be obtained analytically only in special limits. For example, consider the limit of infinitely strong feedback ($k_2 \rightarrow \infty$). In this limit, $\langle x \rangle$ takes the following form (SI Text)

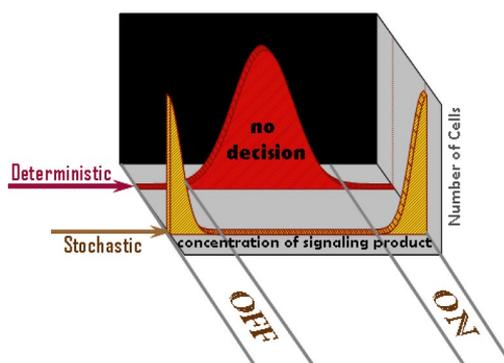


Fig. 5. Stochastic fluctuations can enable cellular decisions. Schematic representation showing that irreversibility, branching, and dueling feedback loops associated with intrinsic time scales, when combined with stochastic effects, can result in distinct functional decisions for each cell. A deterministic treatment would mask this ability of cells to make decisions.

